Geophysical Research Letters

Supporting Information for

Lateral migration patterns toward or away from injection wells for earthquake clusters in Oklahoma

J. A. López-Comino[1,2,3,4] M. Galis[5,6], P. M. Mai[1], X. Chen[7] , D. Stich[2,3]

[1] KAUST, King Abdullah University of Science and Technology, Thuwal (Saudi Arabia). [2] Instituto Andaluz de Geofísica, Universidad de Granada, Granada, Spain. [3] Departamento de Física Teórica y del Cosmos, Universidad de Granada, Granada, Spain. [4] Institute of Earth and Environmental Sciences, University of Potsdam, D-14476 Potsdam-Golm, Germany. [5] Faculty of Mathematics, Physics and Informatics, Comenius University in Bratislava, Slovakia. [6] Earth Science Institute, Slovak Academy of Sciences, Bratislava, Slovakia. [7] ConocoPhillips School of Geology and Geophysics, The University of Oklahoma, Norman, OK, USA

Corresponding author: José Ángel López-Comino (jose.lopezcomino@kaust.edu.sa)

Contents of this file

Figures S1 to S11
Table S1

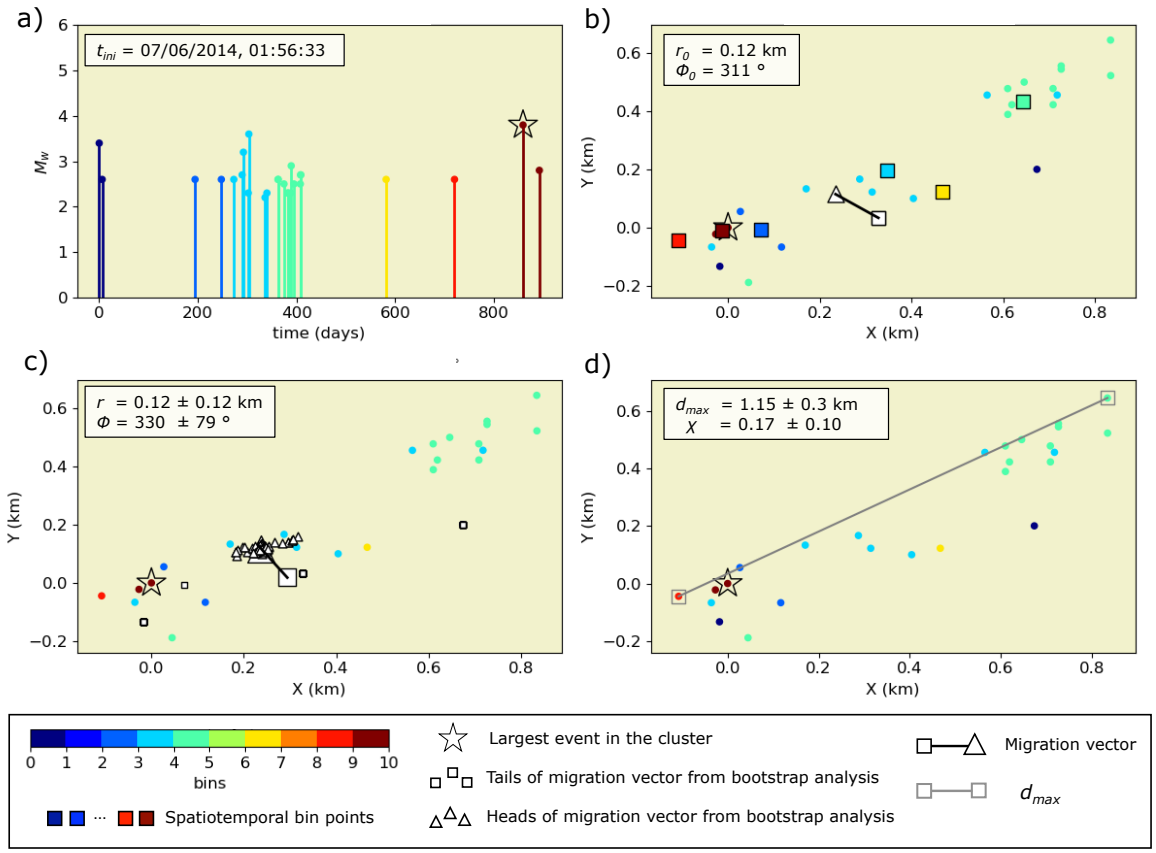

Figure S1. Migration analysis for cluster 17 (see Figure 1) showing results for an unstable migration vector. a) Temporal evolution of the seismic sequence from t_{ini}; the color scale indicates association of seismic events with temporal bins and the star depicts the largest event in the cluster. b) The migration vector (black line) defined from tail (white square) to head (white triangle) and the spatiotemporal evolution of migration (color-coded squares indicate the spatiotemporal bin points). r_0 and Φ_0 represent the length and azimuth of the migration vector calculated using all events in the cluster. c) Bootstrap analysis to calculate the final length r and azimuth Φ of the migration vector and their uncertainties. Small white triangles and small white squares depict the heads and tails of 100 migration vectors for the bootstrap analysis. The final migration vector is depicted by a black line from the tail (large white square) to the head (large white triangle). d) The maximum cluster length (d_{max}) and the migration coefficient (χ) are shown with the uncertainties obtained from the bootstrap analysis. d_{max} (gray line) is defined by the two seismic events farthest from each other (open gray squares).

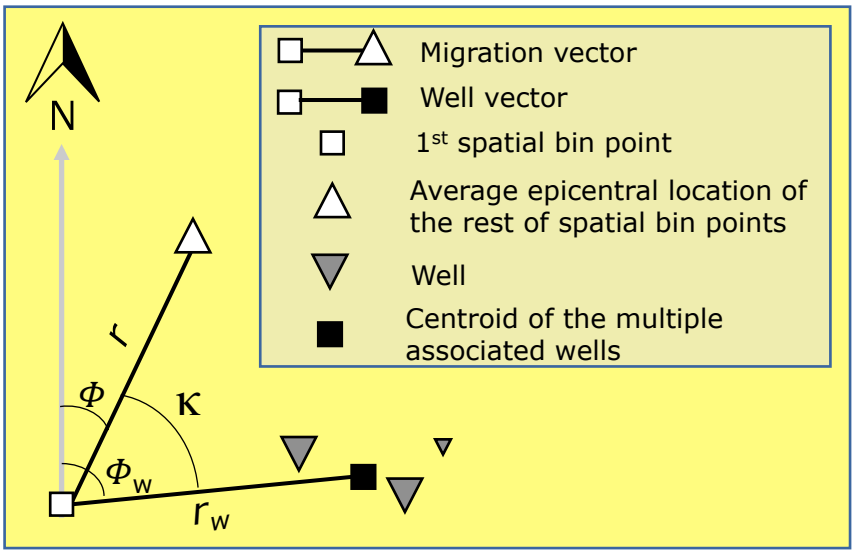

Figure S2. Sketch showing the parameters for calculating the migration and well vector for the comprehensive migration analysis with respect to multiple wells.

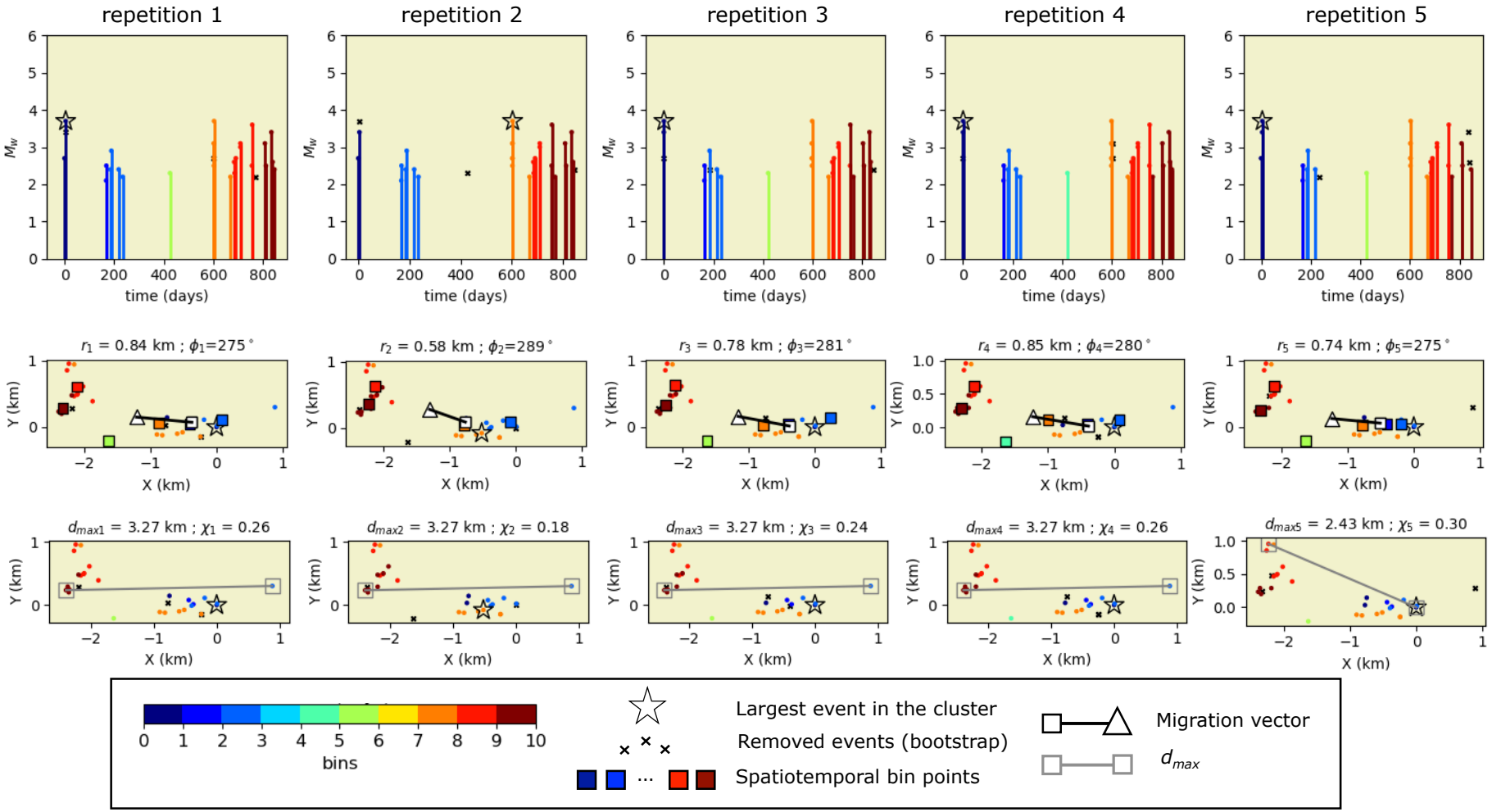

Figure S3. Bootstrap analysis for 5 repetitions (repetitions per columns) to calculate migration parameters for cluster 52. This procedure is repeated 100 times randomly removing the 10% of the events (black x-points). (First row) Temporal evolution of the seismic sequence for each repetition; the color scale indicates different temporal bins associated for each seismic event and the star shows the largest event in the cluster. (Second row) The migration vector (black line) defined from tail (white square) to head (white triangle) and the spatiotemporal evolution of migration (color-coded squares indicate the spatiotemporal bin points). r_i and Φ_i represent the length and azimuth of the migration vector for each *i* repetition. (Third row) The total length (d_{max}) of the cluster (gray line) is defined by the two seismic events farthest from each other (open gray squares) and the migration coefficient (χ) is also shown for each repetition.

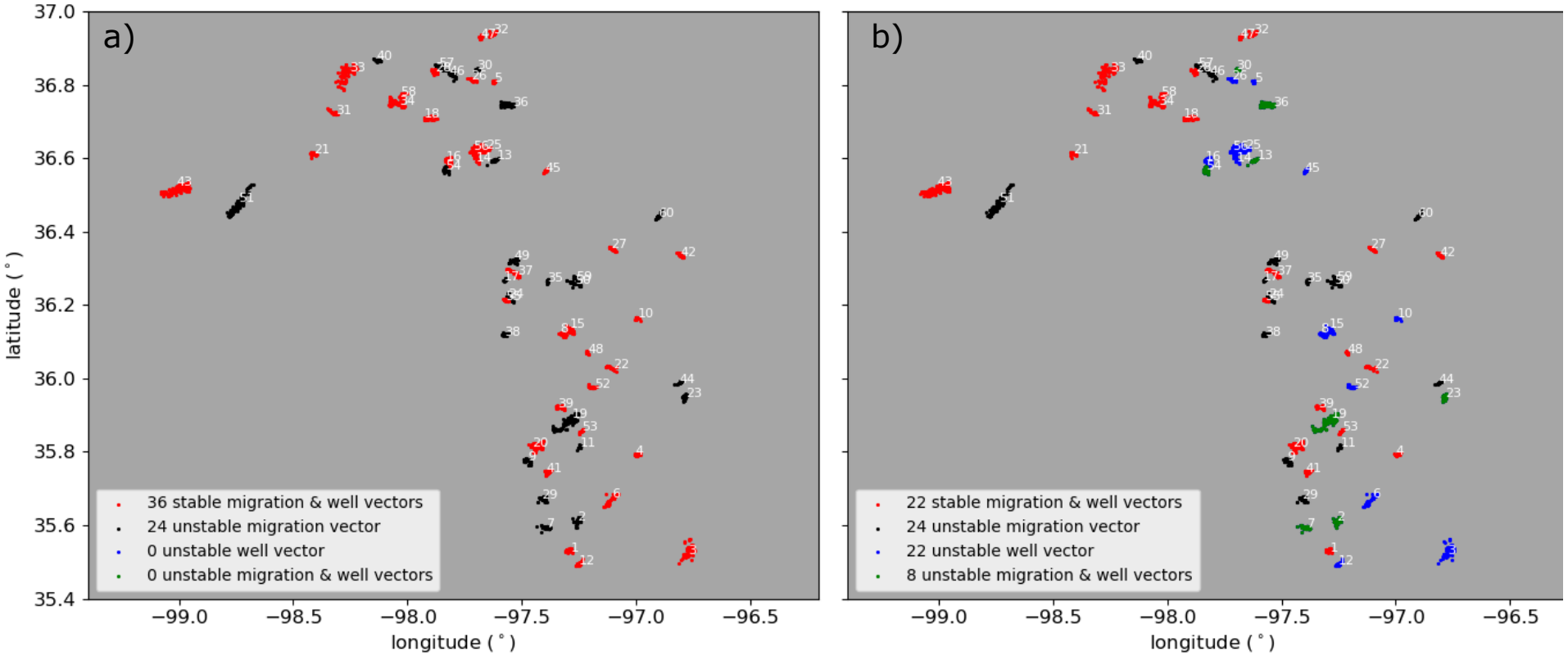

Figure S4. Migration and well vector stability for each cluster (color-coded dots) considering a cumulative volume weighting (a) and an injection rate volume weighting (b). White numbers denote each cluster (see table S1).

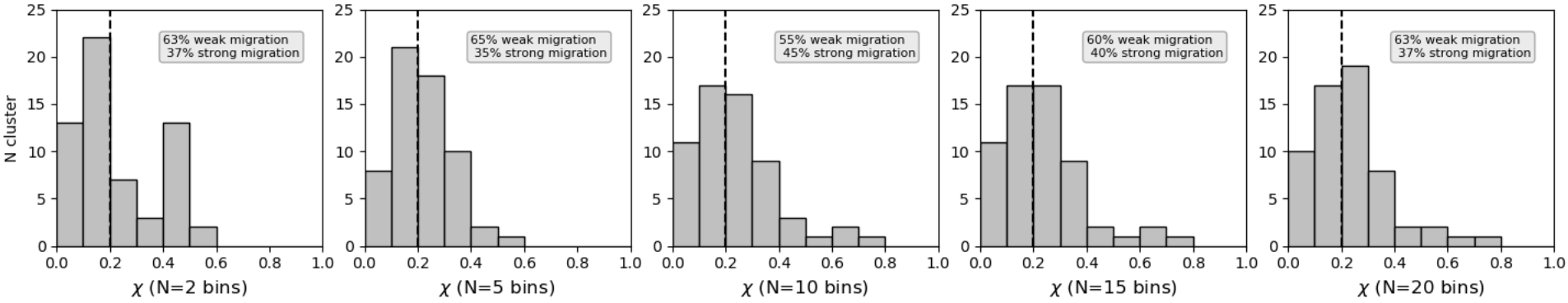

Figure S5. Histograms for the migration coefficient (χ) using different temporal bins (N) in the comprehensive migration analysis. The dashed black lines separates weak ($\chi < 0.2$) and strong ($\chi > 0.2$) migration clusters.

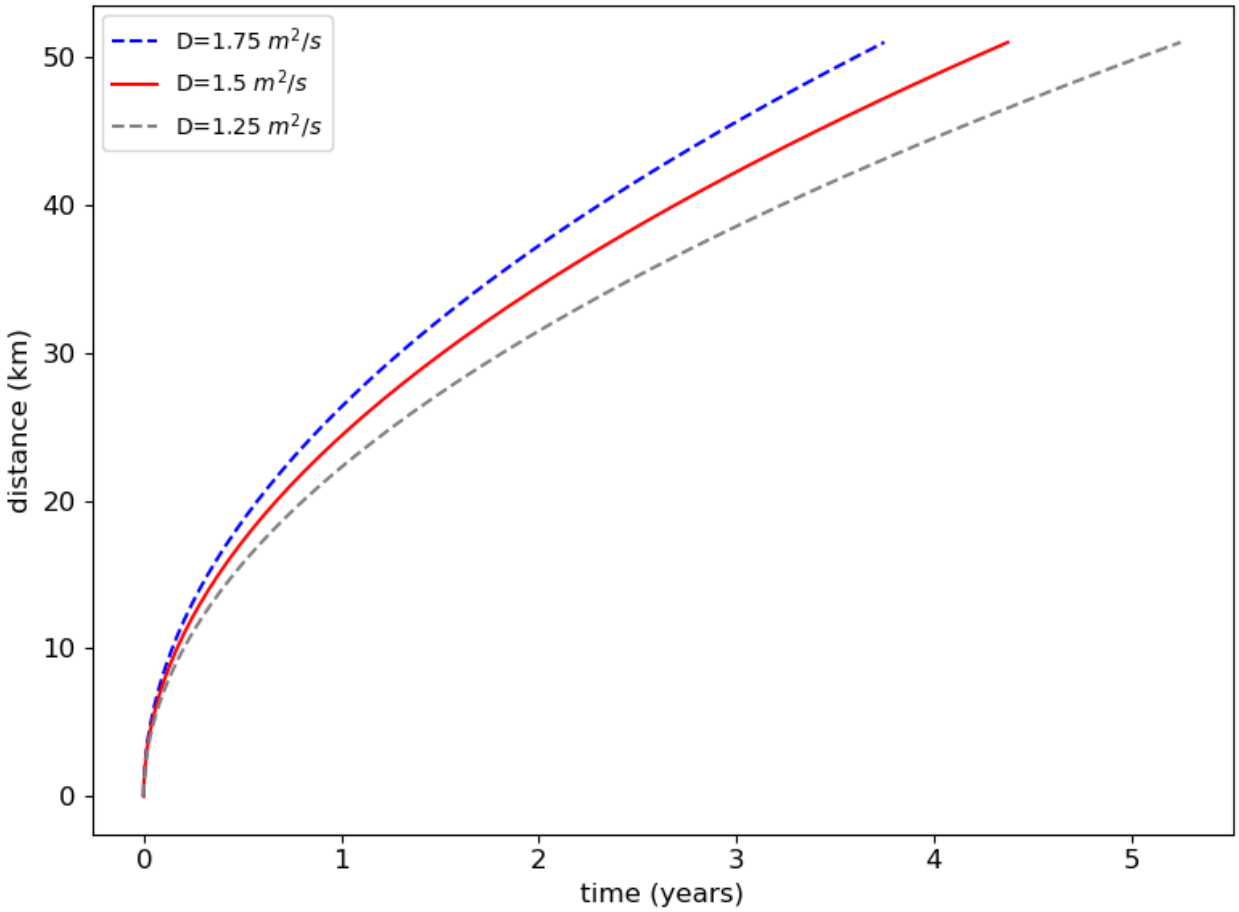

Figure S6. Diffusion fronts according Shapiro et al., 2005 for different diffusion coefficients (D) tested in the comprehensive migration analysis with respect to multiple injection wells.

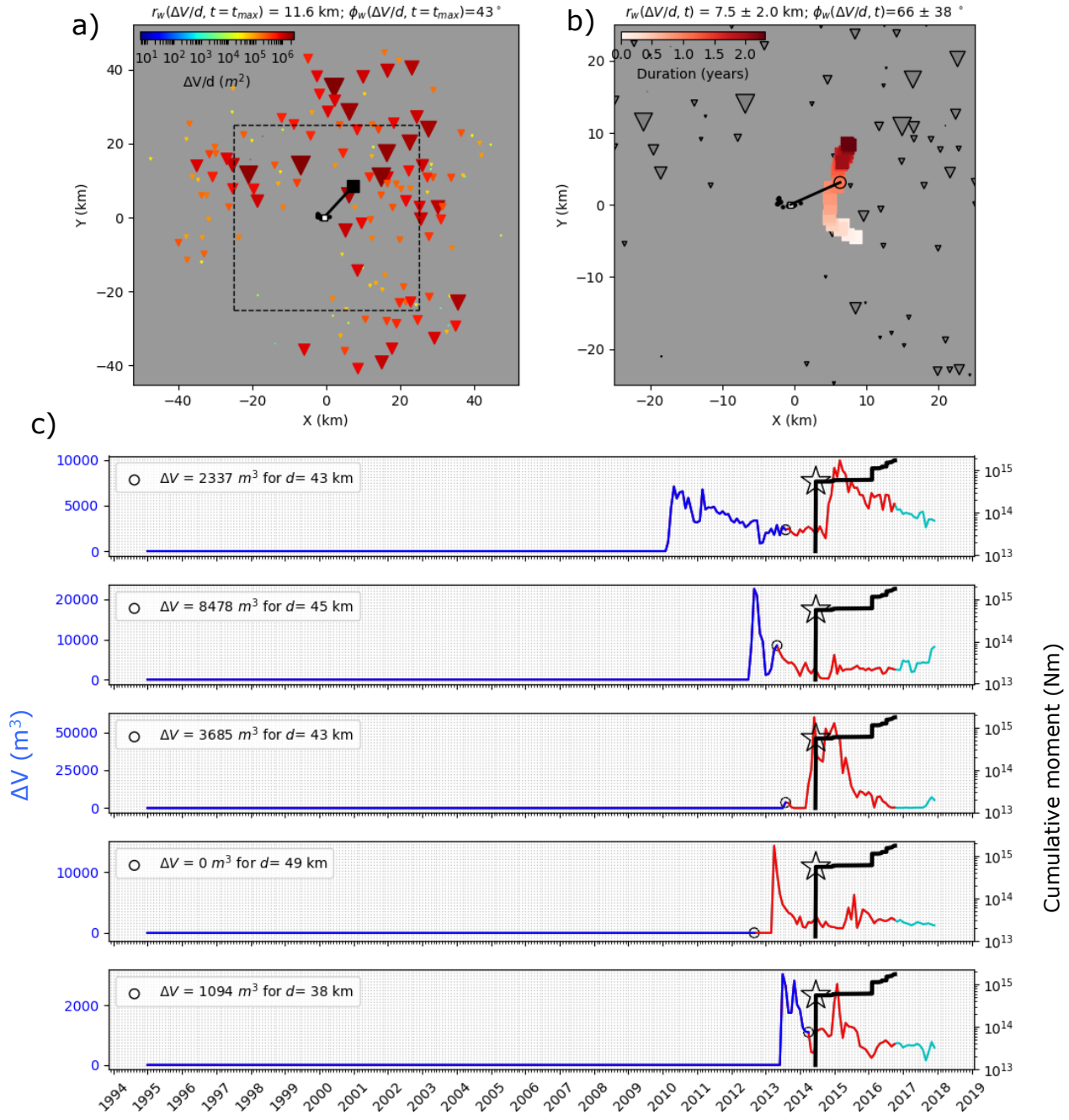

Figure S7. Calculating the well vector for cluster 52 considering the injection rate volume weighting and a diffusion coefficient of 1.5 m^2/s. a) Situation at the final time of the seismic sequence t_{max}. The well vector (black line) is defined from the tail of the migration vector (white square defined in Fig 2c) to the injection midpoint (black square). Length (r_w) and azimuth (Φ_w) of the well vector are indicated in the figure header. Wells (inverted triangles) are scaled (color and size) according $\Delta V(t_{max}-t_D)/d$. b) Location of injection midpoints during the seismic sequence (color-coded squares). The final injection midpoint is shown with an open black circle, the final well vector by the black line. Wells are scaled in size as in a). Only the dashed rectangle from a) is shown. c) Injection rate volumes for five wells associated with the cluster (blue lines) and cumulative seismic moment for the seismic sequence (black line; the largest event is indicated by the star). Red lines indicate the volume that did not affect the cluster due to diffusion constraints, cyan lines indicate data available after the end of seismic sequence. For each well the injection rate volume (ΔV) with respect to t_{max} (open black circle) and the well distance (d) are indicated.

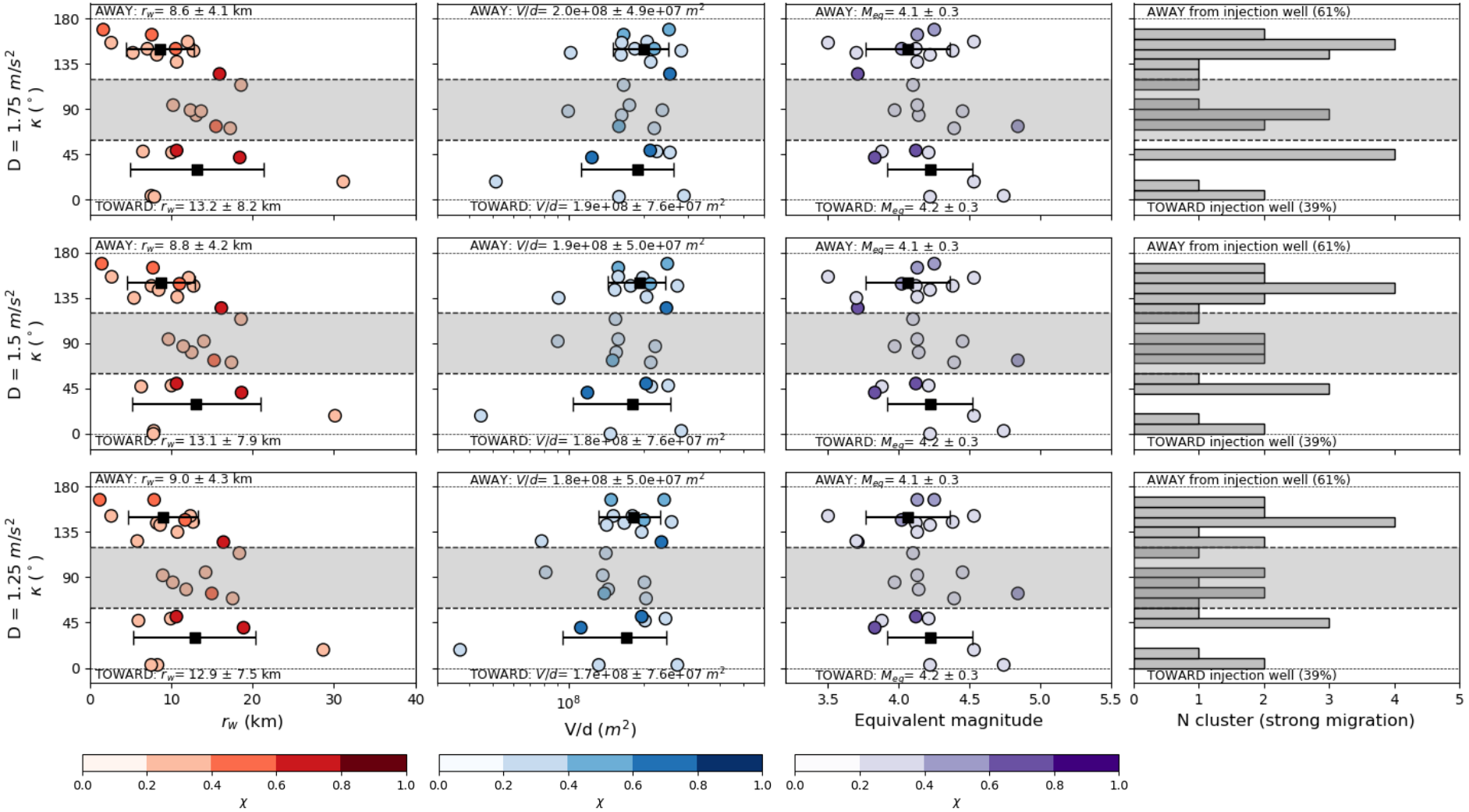

Figure S8. Lateral migration patterns toward or away from injection wells characterized by κ-values using 10 temporal bins in the comprehensive migration analysis and different diffusion coefficients of 1.75 m^2/s (first row), 1.5 m^2/s (second row) and 1.25 m^2/s (third row). κ-values for strong migration clusters ($\chi > 0.2$) are plotted as circles scaled in color according the migration coefficient (χ), considering the cumulative volume weighting. Results are shown for each cluster according to the length of the well vector (first column), the total weights assigned to the multiple associated wells in relation to cumulative injected volumes (second column) and the equivalent magnitude (third column). Average values and error bars (black squares and lines) are indicated for propagation toward ($\kappa < 60°$) and away ($\kappa > 120°$) from the injection point (see labels). Histograms are also shown including percentages values (forth column). Intermediate cases ($60° < \kappa < 120°$) are not considered (gray background separated by black dashed lines).

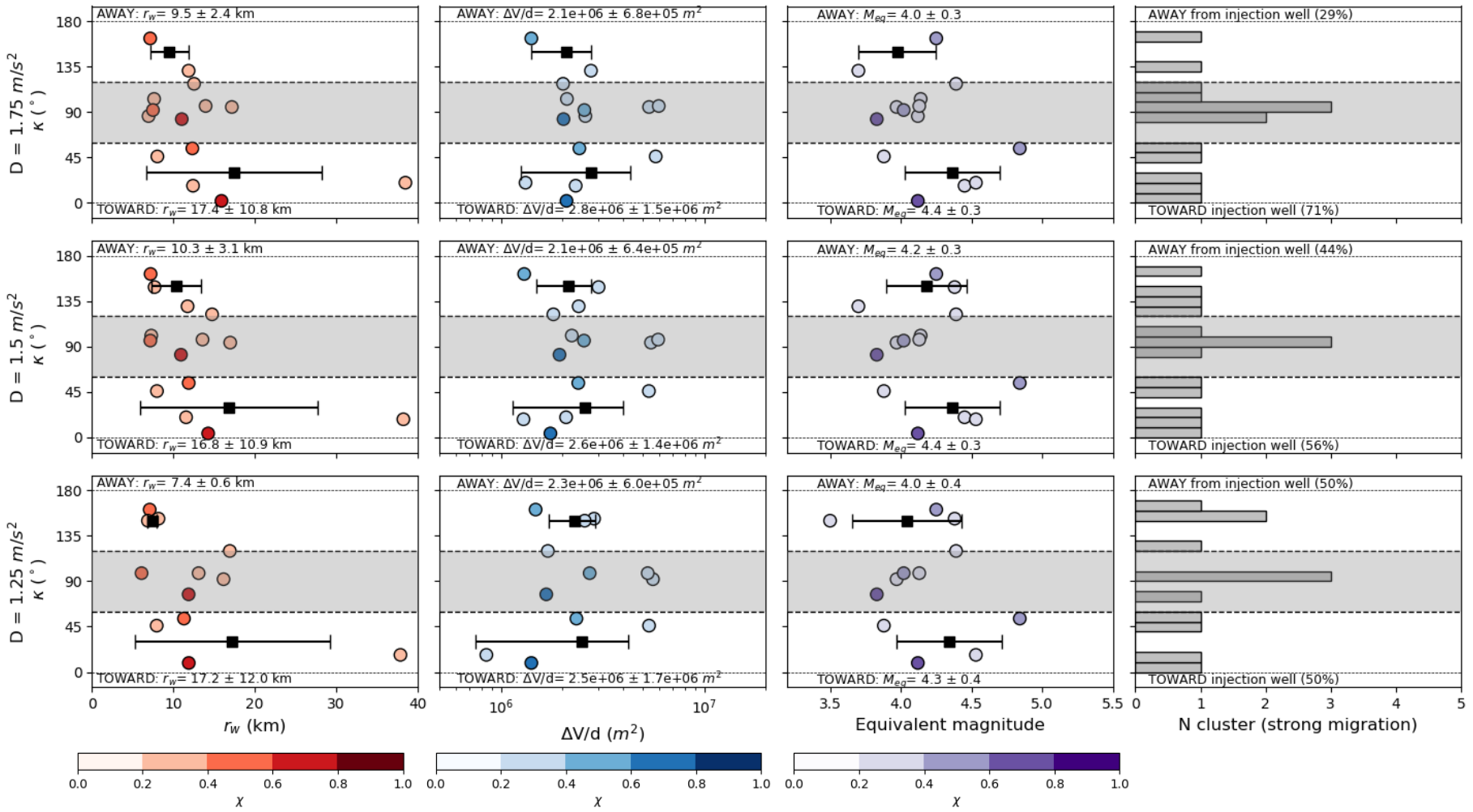

Figure S9. Same as figure S8, but considering injection rate volume weighting. Note that second column show the results according to the total weights assigned to the multiple associated wells in relation to injection rate volumes.

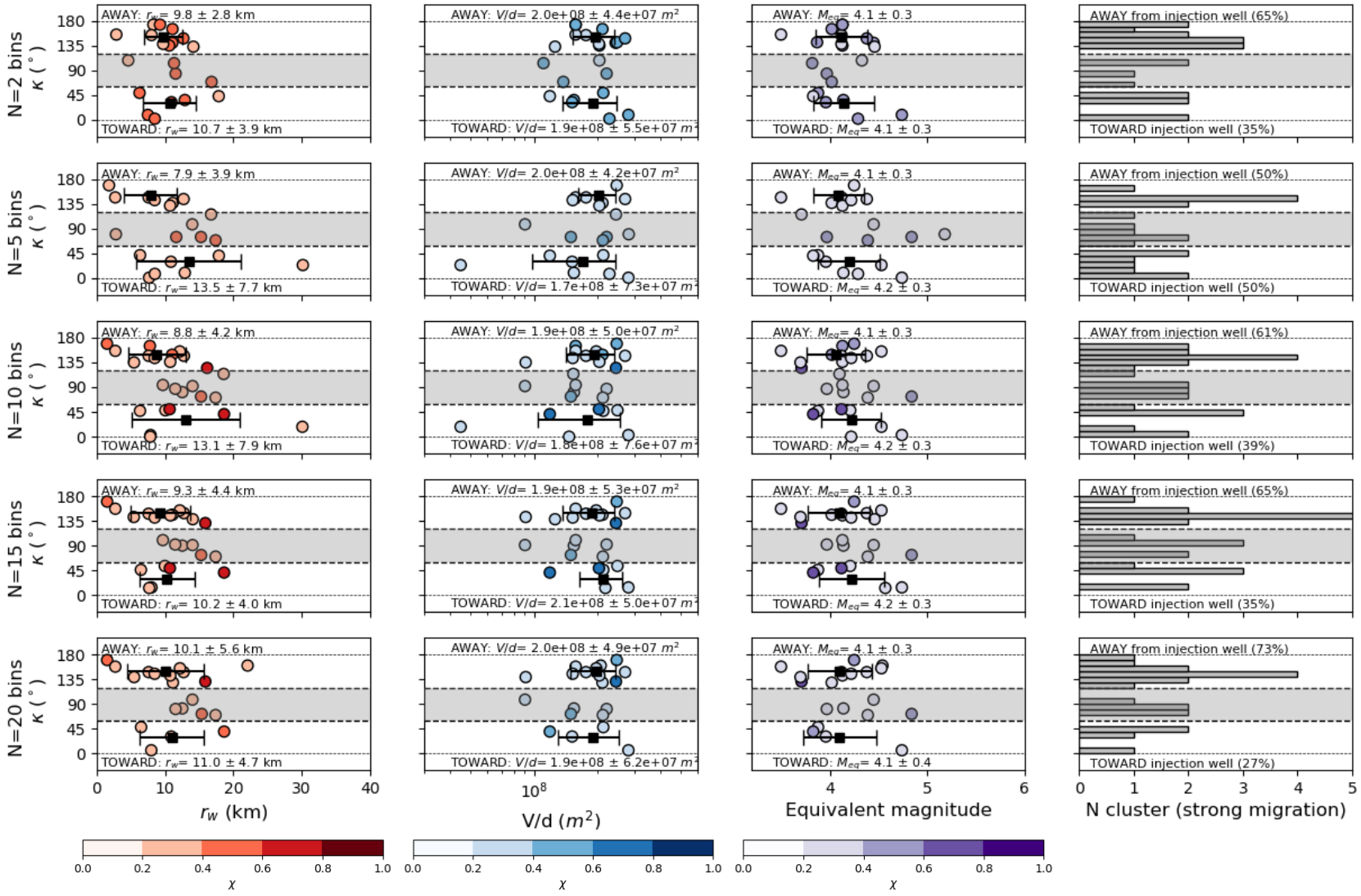

Figure S10. Lateral migration patterns toward or away from injection wells characterized by κ-values using 2 (first row), 5 (second row), 10 (third row), 15 (fourth row) and 20 (fifth row) temporal bins in the comprehensive migration analysis and a coefficient diffusion of 1.5 m^2/s. κ-values for strong migration clusters ($\chi > 0.2$) are plotted as circles scaled in color according the migration coefficient (χ), considering the cumulative volume weighting. Results are shown for each cluster according to the length of the well vector (first column), the total weights assigned to the multiple associated wells in relation to cumulative injected volumes (second column) and the equivalent magnitude (third column). Average values and error bars (black squares and lines) are indicated for propagation toward ($\kappa < 60°$) and away ($\kappa > 120°$) from the injection point (see labels). Histograms are also shown including percentages values (forth column). Intermediate cases ($60° < \kappa < 120°$) are not considered (gray background separated by black dashed lines).

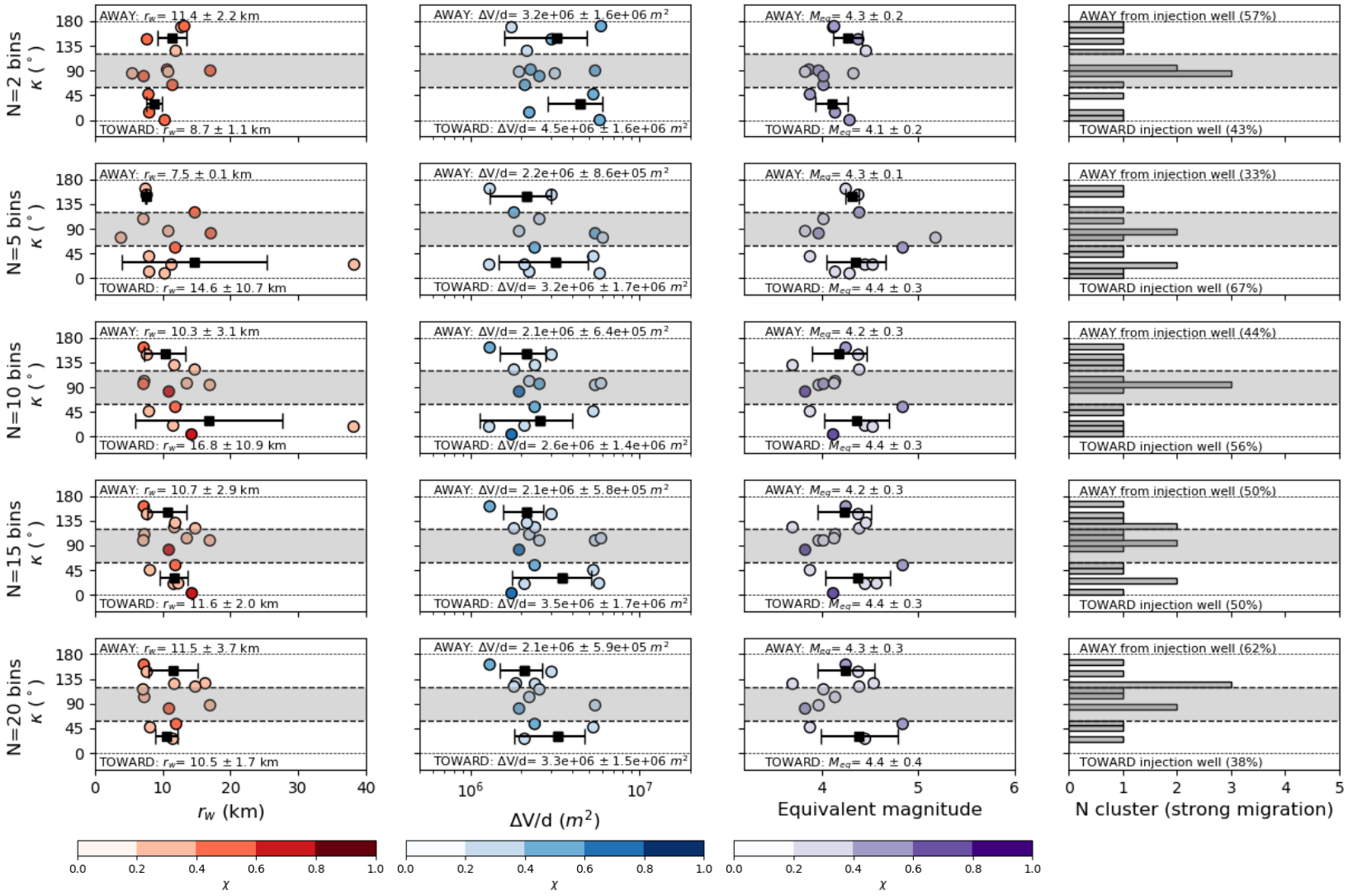

Figure S11. Same as figure S10, but considering injection rate volume weighting. Note that second column show the results according to the total weights assigned to the multiple associated wells in relation to injection rate volumes.

Cluster ID	lon (deg)	lat (deg)	N events	ϕ (deg)	ϕw (deg)		Kappa (deg)		r (km)	dmax (km)	Xi	rw (km)		V/d (m2)	ΔV/d (m2)	Meq (Nm)	Stability (1 = YES & 0 = No)		
					for V weighting	for ΔV weighting	for V weighting	for ΔV weighting				for V weighting	for ΔV weighting				Migration vector	Well vector	
																		for V weighting	for ΔV weighting
1	-97,285	35,528	29	301 ± 9	22 ± 2	42 ± 9	81	101	1,01 ± 0,17	2,74 ± 0,07	0,37 ± 0,06	12,53 ± 0,72	7,27 ± 1,39	1,55E+08	2,23E+06	4,14	1	1	1
2	-97,259	35,613	48	268 ± 37	42 ± 7	116 ± 62	134	152	0,62 ± 0,18	3,52 ± 0,05	0,18 ± 0,05	11,1 ± 1,78	3,87 ± 1,87	2,45E+08	1,76E+06	4,45	0	1	0
3 (Prague)	-96,772	35,522	90	22 ± 17	328 ± 11	93 ± 89	54	71	0,64 ± 0,12	8,36 ± 0,38	0,08 ± 0,01	2,13 ± 0,44	2,18 ± 1,30	2,44E+08	1,16E+06	5,74	1	1	0
4	-97,001	35,792	25	251 ± 3	60 ± 15	89 ± 19	169	162	1,11 ± 0,07	2,50 ± 0,10	0,44 ± 0,04	1,49 ± 0,29	7,19 ± 0,95	2,48E+08	1,30E+06	4,25	1	1	1
5	-97,62	36,809	30	21 ± 18	135 ± 3	137 ± 44	114	116	0,25 ± 0,04	1,06 ± 0,02	0,24 ± 0,03	18,59 ± 3,15	10,72 ± 4,11	1,54E+08	2,52E+06	4,1	1	1	0
6	-97,104	35,675	36	37 ± 10	40 ± 3	158 ± 57	3	121	1,61 ± 0,14	7,10 ± 0,12	0,23 ± 0,02	7,87 ± 0,89	3,38 ± 0,80	2,82E+08	1,74E+06	4,74	1	1	0
7	-97,393	35,593	90	287 ± 39	86 ± 7	154 ± 25	159	133	0,24 ± 0,08	5,07 ± 0,50	0,05 ± 0,01	9,41 ± 0,59	8,65 ± 1,20	2,24E+08	1,10E+06	4,96	0	1	0
8	-97,33	36,124	20	112 ± 14	139 ± 4	24 ± 70	27	88	0,54 ± 0,12	3,07 ± 0,17	0,18 ± 0,05	10,85 ± 1,45	3,55 ± 2,63	1,52E+08	2,40E+06	3,96	1	1	0
9	-97,475	35,775	53	152 ± 67	109 ± 3	140 ± 13	43	12	0,23 ± 0,07	3,34 ± 0,09	0,07 ± 0,02	22,82 ± 0,82	16,84 ± 4,42	2,08E+08	1,86E+06	4,54	0	1	1
10	-96,992	36,165	23	291 ± 11	166 ± 0	160 ± 53	125	131	1,56 ± 0,27	2,19 ± 0,14	0,71 ± 0,10	16,17 ± 1,96	2,10 ± 0,66	2,46E+08	2,53E+06	3,71	1	1	0
11	-97,243	35,814	23	265 ± 26	108 ± 3	156 ± 17	157	109	0,28 ± 0,05	1,78 ± 0,15	0,16 ± 0,02	9,93 ± 0,17	10,63 ± 4,11	2,49E+08	2,27E+06	3,87	0	1	1
12	-97,25	35,494	28	60 ± 21	12 ± 2	309 ± 47	48	111	1,04 ± 0,19	3,41 ± 0,18	0,31 ± 0,05	10,05 ± 0,6	3,69 ± 0,57	2,50E+08	1,28E+06	4,21	1	1	0
13	-97,607	36,596	42	255 ± 89	99 ± 5	66 ± 31	156	171	0,42 ± 0,13	4,41 ± 0,60	0,1 ± 0,02	12,21 ± 1,12	6,62 ± 2,66	1,78E+08	3,28E+06	4,58	0	1	0
14	-97,697	36,591	23	298 ± 19	103 ± 3	46 ± 66	165	108	1,11 ± 0,14	2,64 ± 0,19	0,43 ± 0,04	7,78 ± 1,43	1,37 ± 1,26	1,58E+08	2,77E+06	4,13	1	1	0
15	-97,29	36,138	56	294 ± 5	147 ± 10	19 ± 26	147	85	1,27 ± 0,09	3,77 ± 0,32	0,34 ± 0,04	7,6 ± 1,7	6,22 ± 1,76	1,77E+08	2,51E+06	4,12	1	1	0
16	-97,832	36,594	52	99 ± 18	99 ± 6	46 ± 41	0	53	0,87 ± 0,16	3,03 ± 0,05	0,29 ± 0,06	7,83 ± 2,24	2,11 ± 1,29	1,47E+08	3,28E+06	4,22	1	1	0
17	-97,578	36,267	26	321 ± 79	36 ± 3	49 ± 11	80	93	0,12 ± 0,13	1,16 ± 0,03	0,19 ± 0,11	17,24 ± 1,22	11,87 ± 2,86	1,36E+08	2,27E+06	4,03	0	1	1
18	-97,927	36,71	38	257 ± 19	263 ± 12	291 ± 13	6	34	0,91 ± 0,14	5,18 ± 0,08	0,18 ± 0,03	5,78 ± 0,59	10,22 ± 2,03	1,17E+08	4,68E+06	4,78	1	1	1
19	-97,279	35,891	123	197 ± 41	104 ± 2	77 ± 39	93	120	0,36 ± 0,10	10,86 ± 0,03	0,03 ± 0,01	16,73 ± 0,4	13,01 ± 3,84	1,90E+08	1,62E+06	4,81	0	1	0
20 (Guthrie)	-97,452	35,815	157	288 ± 11	114 ± 2	152 ± 9	174	136	0,81 ± 0,12	5,82 ± 0,21	0,14 ± 0,02	20,49 ± 0,8	13,16 ± 3,89	2,04E+08	1,97E+06	4,7	1	1	1
21	-98,411	36,612	21	271 ± 10	358 ± 5	5 ± 3	87	94	0,79 ± 0,07	2,43 ± 0,06	0,32 ± 0,03	11,49 ± 1,47	16,97 ± 1,55	2,22E+08	5,47E+06	3,97	1	1	1
22	-97,1	36,027	29	292 ± 4	145 ± 3	81 ± 21	147	149	1,05 ± 0,33	4,62 ± 0,11	0,23 ± 0,07	12,76 ± 0,64	7,68 ± 0,41	2,72E+08	3,02E+06	4,38	1	1	1
23	-96,784	35,948	33	334 ± 50	228 ± 5	323 ± 37	106	11	0,75 ± 0,12	2,46 ± 0,04	0,31 ± 0,05	5,73 ± 0,46	4,05 ± 1,34	2,99E+08	2,59E+06	4,19	0	1	0
24	-97,56	36,22	20	49 ± 79	50 ± 1	46 ± 7	1	3	0,64 ± 0,12	3,46 ± 0,07	0,2 ± 0,03	17,02 ± 0,79	11,60 ± 2,01	1,38E+08	2,10E+06	4,02	0	1	1
25	-97,657	36,626	89	258 ± 2	103 ± 5	74 ± 33	155	176	1,95 ± 0,13	6,93 ± 0,13	0,28 ± 0,02	12,16 ± 1,49	6,39 ± 3,42	1,98E+08	2,75E+06	4,53	1	1	0
26	-97,72	36,813	47	109 ± 15	140 ± 6	202 ± 68	31	93	0,46 ± 0,12	3,56 ± 0,07	0,13 ± 0,03	10,2 ± 1,32	4,26 ± 2,44	1,86E+08	3,92E+06	4,44	1	1	0
27	-97,112	36,355	32	118 ± 11	289 ± 3	267 ± 13	171	149	0,43 ± 0,13	2,93 ± 0,06	0,15 ± 0,04	10,24 ± 0,69	5,82 ± 0,99	1,82E+08	2,78E+06	4,33	1	1	1
28	-97,879	36,837	53	149 ± 18	265 ± 9	287 ± 7	116	138	0,46 ± 0,04	2,46 ± 0,00	0,19 ± 0,01	8,16 ± 0,61	12,99 ± 1,82	1,15E+08	3,84E+06	4,06	1	1	1
29	-97,412	35,672	63	66 ± 28	97 ± 6	152 ± 19	31	86	0,27 ± 0,13	3,91 ± 0,09	0,07 ± 0,03	14,47 ± 0,62	13,00 ± 2,45	2,26E+08	1,47E+06	4,83	0	1	1
30	-97,697	36,843	20	108 ± 90	143 ± 6	209 ± 69	35	101	0,06 ± 0,04	1,42 ± 0,09	0,06 ± 0,03	10,41 ± 1,12	5,10 ± 2,40	1,72E+08	3,63E+06	3,92	0	1	0
31	-98,313	36,721	24	297 ± 4	344 ± 0	343 ± 4	47	46	1,29 ± 0,18	4,21 ± 0,12	0,31 ± 0,04	6,33 ± 0,23	7,97 ± 0,21	2,14E+08	5,34E+06	3,88	1	1	1
32	-97,625	36,94	52	238 ± 5	146 ± 4	218 ± 14	92	20	0,98 ± 0,09	3,42 ± 0,20	0,29 ± 0,03	14,03 ± 0,59	11,55 ± 0,74	9,06E+07	2,09E+06	4,45	1	1	1
33	-98,251	36,836	76	193 ± 19	307 ± 11	294 ± 11	114	101	1,07 ± 0,43	9,56 ± 0,05	0,11 ± 0,05	2,38 ± 0,18	3,28 ± 0,47	2,83E+08	6,08E+06	5,18	1	1	1
34	-98,038	36,745	98	278 ± 6	290 ± 6	298 ± 6	12	20	1,30 ± 0,07	6,37 ± 0,09	0,2 ± 0,01	7,67 ± 1,14	12,30 ± 1,27	2,19E+08	5,77E+06	4,57	1	1	1
35	-97,391	36,265	27	49 ± 90	26 ± 1	33 ± 17	23	16	0,02 ± 0,07	1,51 ± 0,05	0,05 ± 0,05	8,07 ± 0,1	7,09 ± 0,58	1,74E+08	2,83E+06	3,94	0	1	1
36	-97,538	36,742	95	5 ± 87	129 ± 2	140 ± 34	124	135	0,45 ± 0,05	5,29 ± 0,04	0,1 ± 0,01	16,28 ± 0,93	10,49 ± 1,52	1,76E+08	2,03E+06	4,24	0	1	0
37	-97,522	36,281	130	114 ± 2	41 ± 4	60 ± 12	73	54	2,91 ± 0,19	5,57 ± 0,07	0,52 ± 0,04	15,28 ± 0,93	11,87 ± 2,78	1,50E+08	2,40E+06	4,84	1	1	1
38	-97,575	36,116	22	355 ± 46	83 ± 1	56 ± 7	88	61	0,30 ± 0,08	2,86 ± 0,03	0,11 ± 0,03	15,11 ± 0,45	8,50 ± 0,91	1,08E+08	1,27E+06	4,45	0	1	1
39	-97,341	35,922	36	112 ± 11	111 ± 1	56 ± 19	1	56	0,51 ± 0,13	3,36 ± 0,05	0,15 ± 0,04	19,66 ± 0,38	8,80 ± 1,05	1,66E+08	1,32E+06	4,62	1	1	1
40	-98,135	36,868	23	275 ± 86	277 ± 1	275 ± 3	2	0	0,21 ± 0,09	2,89 ± 0,02	0,08 ± 0,03	8,3 ± 0,28	10,10 ± 0,31	2,29E+08	5,83E+06	4,29	0	1	1
41	-97,394	35,744	52	30 ± 7	101 ± 2	152 ± 13	71	122	1,14 ± 0,06	2,90 ± 0,13	0,39 ± 0,02	17,41 ± 0,26	14,74 ± 2,88	2,13E+08	1,81E+06	4,39	1	1	1
42	-96,805	36,334	20	121 ± 4	162 ± 1	203 ± 3	41	82	1,81 ± 0,09	2,93 ± 0,02	0,62 ± 0,03	18,65 ± 0,45	10,92 ± 0,20	1,19E+08	1,94E+06	3,83	1	1	1
43 (Woodward)	-99,008	36,525	176	65 ± 11	47 ± 1	47 ± 7	18	18	2,57 ± 0,29	11,50 ± 0,13	0,22 ± 0,03	30,13 ± 1,26	38,24 ± 1,07	4,47E+07	1,29E+06	4,53	1	1	1
44 (Cushing)	-96,811	35,988	27	253 ± 84	202 ± 2	310 ± 14	51	57	0,42 ± 0,19	3,23 ± 0,30	0,14 ± 0,05	6,96 ± 0,48	3,15 ± 0,58	3,09E+08	2,47E+06	5,15	0	1	1
45	-97,397	36,564	27	232 ± 10	76 ± 1	21 ± 73	156	149	0,56 ± 0,06	1,89 ± 0,09	0,3 ± 0,04	2,71 ± 0,06	1,63 ± 1,86	1,58E+08	2,08E+06	3,5	1	1	0
46	-97,815	36,828	41	98 ± 29	258 ± 10	275 ± 12	160	177	0,36 ± 0,18	5,37 ± 0,11	0,07 ± 0,03	7,09 ± 0,91	12,17 ± 1,71	1,44E+08	4,66E+06	4,5	0	1	1
47	-97,68	36,928	27	24 ± 13	159 ± 7	254 ± 4	135	130	0,54 ± 0,07	1,49 ± 0,11	0,37 ± 0,03	5,45 ± 0,25	11,73 ± 1,79	9,13E+07	2,41E+06	3,7	1	1	1
48	-97,211	36,069	20	298 ± 9	149 ± 2	34 ± 8	149	96	0,47 ± 0,04	1,17 ± 0,01	0,41 ± 0,03	11,03 ± 0,54	7,16 ± 0,43	2,12E+08	2,56E+06	4,02	1	1	1
49	-97,535	36,324	55	205 ± 67	27 ± 3	50 ± 15	178	155	0,21 ± 0,11	4,25 ± 0,07	0,06 ± 0,02	12,82 ± 0,42	10,21 ± 1,99	1,45E+08	2,48E+06	4,47	0	1	1
50	-97,268	36,259	33	116 ± 89	4 ± 6	28 ± 12	112	88	0,50 ± 0,21	5,66 ± 0,01	0,09 ± 0,04	4,67 ± 0,05	5,50 ± 0,81	2,05E+08	3,16E+06	4,33	0	1	1
51 (Fairview)	-98,738	36,48	148	269 ± 25	19 ± 3	23 ± 6	110	114	1,67 ± 0,23	13,69 ± 0,18	0,12 ± 0,02	24,84 ± 1,19	28,83 ± 1,60	7,43E+07	2,54E+06	5,31	0	1	1
52	-97,183	35,975	30	278 ± 11	142 ± 4	66 ± 38	136	148	0,69 ± 0,11	3,20 ± 0,24	0,22 ± 0,04	10,76 ± 0,58	7,51 ± 1,99	2,05E+08	2,14E+06	4,13	1	1	0
53	-97,234	35,858	21	46 ± 1	96 ± 1	50 ± 6	50	4	1,39 ± 0,09	2,23 ± 0,06	0,63 ± 0,03	10,67 ± 0	14,26 ± 0,56	2,04E+08	1,75E+06	4,12	1	1	1
54	-97,833	36,568	26	72 ± 62	94 ± 5	61 ± 26	22	11	0,88 ± 0,09	2,63 ± 0,14	0,38 ± 0,04	12,29 ± 1,89	6,25 ± 3,71	1,11E+08	2,78E+06	3,82	0	1	0
55	-97,572	36,214	28	275 ± 8	54 ± 1	47 ± 8	139	132	0,39 ± 0,06	1,93 ± 0,05	0,2 ± 0,03	14,07 ± 0,38	11,86 ± 2,72	1,26E+08	2,16E+06	4,46	1	1	1
56	-97,714	36,621	44	269 ± 8	126 ± 3	147 ± 86	143	122	1,55 ± 0,21	5,19 ± 0,04	0,3 ± 0,04	8,48 ± 1,61	1,48 ± 0,97	1,53E+08	2,98E+06	4,22	1	1	0
57	-97,865	36,849	29	108 ± 90	263 ± 13	283 ± 11	155	175	0,35 ± 0,10	2,71 ± 0,10	0,16 ± 0,04	9,1 ± 0,98	13,65 ± 2,37	1,41E+08	4,51E+06	4,11	0	1	1
58	-98,03	36,771	20	192 ± 13	286 ± 1	289 ± 4	94	97	0,74 ± 0,07	3,03 ± 0,11	0,25 ± 0,02	9,68 ± 0,56	13,57 ± 0,47	1,58E+08	5,93E+06	4,13	1	1	1
59	-97,259	36,268	35	106 ± 86	356 ± 18	29 ± 20	110	77	0,52 ± 0,13	2,41 ± 0,12	0,23 ± 0,06	3,72 ± 0,13	5,69 ± 1,76	2,05E+08	3,05E+06	4,12	0	1	1
60	-96,904	36,441	27	212 ± 90	266 ± 1	248 ± 2	54	36	0,94 ± 0,44	3,47 ± 0,13	0,28 ± 0,12	13,87 ± 0,08	16,43 ± 1,00	1,38E+08	2,44E+06	4,15	0	1	1
															Sum stable cases		36	60	38

Table S1. Parameters derived from the comprehensive migration analysis with respect to multiple injection wells for 60 cluster considered in Oklahoma using 10 temporal bins and a diffusion coefficient of 1.5 m^2/s.